13

Quantitative Analysis of Film Structures with a Diffuse Interface Studied by Auger Electron Spectroscopy

© V.E. Remele, M.A. Mittsev, M.V. Kuzmin

Ioffe Institute,
St. Petersburg, Russia

E-mail: m.kuzmin@mail.ioffe.ru

Received June 25, 2023
Revised June 25, 2023
Accepted July 3, 2023

A model is proposed for interpreting the results of Auger electron spectroscopy in the case of film systems with reactive interfaces. A quantitative relationship has been established between the parameters of the transition layer and the shape of dependences of the Auger signal of the substrate on the film thickness in such systems. The model was tested for three rare-earth metal (Yb, Sm, Gd) —Si(111) interfaces. Quantitative data have been obtained concerning their structure and stoichiometric composition, as well as the dependence of these characteristics on the thermodynamic properties of the studied rare earth metals.

Keywords: surface, thin films, interface, Auger electron spectroscopy, rare-earth metals, silicon.

DOI: 10.61011/PSS.2023.09.57122.89

1. Introduction

Currently, the Auger electron spectroscopy (AES) is one of the most informative methods of thin-film structure investigations [1]. Thus, for example, AES may be used to get the information about thin film growth mechanisms within the thickness l range from $\sim 10^{-1}$ to 10^3 Å. Classification of such mechanisms is usually limited to three main cases: *a*) island growth beginning from minor coatings (Vollmer–Weber mechanism, VW), *b*) layer-by-layer or two-dimensional growth (Frank–van der Merve mechanism, FM) and *c*) layer-by-layer growth alternated with island growth (Stranski–Krastanov mechanism, SK) [1,2]. Film structures, where the VW and SK mechanisms are implemented, may include epitaxial „film A_3B_5 — silicon substrate“ type systems [3] and Ge–Si [4], respectively. The layer-by-layer growth mode, in turn, is observed, in particular, for such metal-film systems as Pb–Ag(111) [5], Na–W(100) [6] and Pd–W(110) [7].

Despite the convenience of the classification shown above, it does not always adequately describe the thin film growth mechanism. A rare-earth metal (REM) — silicon film structure class is one of such cases [8,9]. The study of these systems is currently very important mainly because they can form compound, in particular, REM disilicides that have interesting physical and chemical properties [10–19]. It has been shown before [8] that mixing or, basically, substrate atom diffusion into the growing film may occur at the REM–Si interfaces even at room temperature. Mixing results in formation of a transition layer formed by the metal and semiconductor atoms, and the silicon crystal and metal film interface is transformed rom a chemically abrupt to diffusion one. In the experimental investigations [20–28], formation of a transition layer in the REM–silicon structures was followed by a typical feature in the form of an „shoulder“ on the substrate Auger signal intensity I vs. the amount of evaporated material (for details see Section 3 and 4). Until now, interpretation of similar dependences has been carried out qualitatively only, because not quantitative analysis model was reported. Therefore, extremely little reliable information regarding the structure and mechanism of REM–Si interfacing at room temperature has been published. Moreover, transition layer thickness and stoichiometric composition as well as the way hoe these properties depend on the population of $4f$-shell of REM atoms are not understood. Apparently, such information is important for understanding silicide formation mechanisms in REM–silicon structures.

An attempt to remove the gaps mentioned above has been made herein. a model is offered herein to allow qualitative description of AES findings for REM–silicon film structures with diffusion interfaces at room temperature. This model has been tested for three systems: Yb–Si(111) [23], Sm–Si(111) [26] and Gd–Si(111) [21]. The addressed model may be also used or other film structures, where the substrate atoms diffuse into the growing film.

2. Model

The model is based on the research findings [8,29]. According to [29], the deposited metal film is grown layer-by-layer in Yb–Si(111) structures at room temperature and the mixing rate depends on the experiment conditions. According to [8], to start such mixing, the REM film shall reach the critical thickness l_0. According to these findings, formations of REM–Si interface shall be assumed to take place in three stages. At the first stage, at thicknesses $l < l_0$ (Figure 1, *a*), the film grows layer-by-layer and the

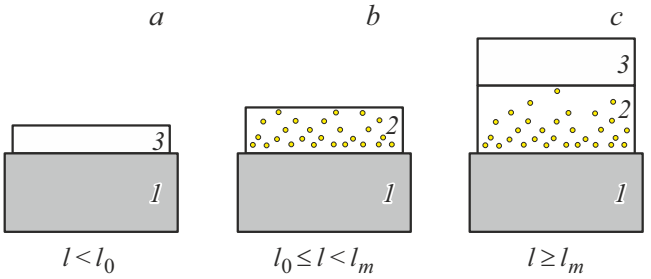

Figure 1. Three REM–silicon interface formation stages. Numbers denote: *1* — silicon substrate, *2* — transition layer, *3* — metallic film.

substrate atoms are not diffused in it. At these l values, the interface is chemically sharp and no transition layer is available. with increasing film thickness and when $l = l_0$ is achieved, the substrate atoms start diffusing into it resulting in qualitative change in the interface properties: a transition layer is formed by the deposited metal and silicon (second stage) atoms. Due to the limited mobility of Si atoms in the REM film at room temperature [8], the transition layer thickness is finite and pure metal starts growing (third stage) on the surface at $l = l_m$. Last two film structure growing stages, i. e. $l_0 \le l < l_m$ and $l \ge l_m$ cases, are schematically shown in Figure 1, *b* and 1, *c*, respectively.

Define the expression for substrate atom Auger signal I vs. the thickness l of the growing film for the structures shown in Figure 1. For convenience, the influence of the silicon atoms diffused into the film (impurity atoms) over the total film thickness and free electron transit length λ will not be considered initially. This approach is apparently true, if the concentration of such atoms is much lower than that of the metal atoms in one film monolayer (ML). In this case, $I(l)$ is written as follows:

$$I(l) = \begin{cases} I_0 \exp\left(-\dfrac{l}{\lambda \cdot \cos\vartheta}\right), & l < l_0, \\ I_0 \exp\left(-\dfrac{l}{\lambda \cdot \cos\vartheta}\right) + I'(l), & l \ge l_0, \end{cases} \tag{1}$$

where I_0 is the Auger signal of the substrate before metal film deposition, I' is the Auger signal from the impurity atoms in the film and ϑ is the Auger electron collection angle counted from the normal to surface. To find the expression for $I'(l)$, consider the silicon impurity atom distribution in the metal film. For this, use the second Fick's equation for one-dimensional case in stationary conditions

$$\frac{d^2N(z)}{dz^2} = 0,$$

where N is the Si atom concentration in the film and z is the coordinate along the normal to surface. To solve this equation, proceed from the continuous quantity $N(z)$ to discrete quantity $N(i)$ (i is the serial number of the metal film layer counted from the substrate interface) and substitute the following boundary conditions: $N(i) \equiv N_0$ at $i = 1$ and $N(i) \equiv 0$ at $i = l_m$. Then we get the following expression

$$N(i) = -\frac{N_0}{l_m - 1}\, i + \frac{N_0 l_m}{l_m - 1} \equiv N_0 f(i), \tag{2}$$

where $f(i)$ is the function of silicon impurity distribution in the film. Due to the physical restrictions, it is defined by the expression

$$f(i) = \begin{cases} -\dfrac{1}{l_m - 1}\, i + \dfrac{l_m}{l_m - 1}, & i < l_m, \\ 0, & i \ge l_m. \end{cases} \tag{3}$$

Express N_0 in terms of atom concentration N_{ML} in one ML of the silicon substrate (for Si(111), $N_{ML} = 7.84 \cdot 10^{14}\,\mathrm{cm}^{-2}$) as follows:

$$N_0 = \gamma N_{ML}, \tag{4}$$

where γ is the constant coefficient defined by the interface reactivity (mixing parameter). Then, considering (3) and (4), the Auger signal rate from the impurity atoms in the i-th layer of the metal film may be written as

$$I'_i = \gamma f(i) I_{ML} \exp\left(-\frac{l - i}{\lambda \cdot \cos\vartheta}\right), \tag{5}$$

where I_{ML} is the Auger signal strength from 1 ML silicon atoms (top atomic layer of the pure substrate). To find I_{ML}, expand I_0 (may be measured directly in the experiment) into Taylor's series:

$$I_0 = I_{ML} + I_{ML} \exp\left(-\frac{d_S}{\lambda_S \cos\vartheta}\right)$$

$$+ I_{ML} \exp\left(-\frac{2d_S}{\lambda_S \cos\vartheta}\right) + \ldots = \sum_{j=1}^{\infty} I_{ML} \exp\left(-\frac{(j-1) \cdot d_S}{\lambda_S \cos\vartheta}\right), \tag{6}$$

where d_S is the thickness of one substrate atom monolayer and λ_S is the free Auger electron transit length in the substrate. From expression (6) we get

$$I_{ML} = I_0 \left(1 - \exp\left(-\frac{d_S}{\lambda_S \cdot \cos\vartheta}\right)\right). \tag{7}$$

Now determine $I'(l)$ for film thickness l. It is equal to

$$I'(l) = \sum_{i=1}^{l} I'_i = \sum_{i=1}^{l} \gamma f(i) I_{ML} \exp\left(-\frac{l - i}{\lambda \cdot \cos\vartheta}\right). \tag{8}$$

Substituting (8) into (1), find the expression for the substrate Auger signal rate I as function of the film thickness l:

$$I(l) = \begin{cases} I_0 \exp\left(-\dfrac{l}{\lambda \cdot \cos\vartheta}\right), & l < l_0, \\ I_0 \exp\left(-\dfrac{l}{\lambda \cdot \cos\vartheta}\right) & \\ + \sum\limits_{i=1}^{l} \gamma f(i) I_{ML} \exp\left(-\dfrac{l - i}{\lambda \cdot \cos\vartheta}\right), & l \ge l_0. \end{cases} \tag{9}$$

As mentioned above, expression (9) is applicable when condition $\gamma \ll 1$ is satisfied. A more universal case, when the mixing parameter has an arbitrary value, will be discussed below. Dissolution of silicon atoms in the metal film (at $l \geq l_0$) will be apparently followed by the increase in the actual film thickness, which, in turn, shall result in the change of substrate screening conditions by the growing film. And the actual film thickness l' may be written as

$$l' = l + \sum_{i=1}^{l} \gamma f(i) d_S = \sum_{i=1}^{l} d(i), \qquad (10)$$

where $d(i) = d + \gamma f(i) d_S$ is the effective thickness of the i-th layer of such film.

In addition to the actual film thickness increase, substrate atom dissolution in it shall result in change of the free electron transit length, because the electrons will be exposed to inelastic interactions not only with the metal atoms, but also with the impurity Si atoms. Assume that the free transit length λ' in such film depends on the distribution function $f(i)$. Then it can be written as

$$\lambda'(i) = \frac{1}{1 + \gamma f(i)} \lambda + \frac{\gamma f(i)}{1 + \gamma f(i)} \lambda_S. \qquad (11)$$

Thus, considering (10) and (11), expression (9) can be rewritten in general terms

$$I(l) = \begin{cases} I_0 \exp\left(-\dfrac{l}{\lambda \cdot \cos\vartheta}\right), & l < l_0, \\ I_0 \prod\limits_{j=1}^{l} \exp\left(-\dfrac{d(j)}{\lambda'(j) \cdot \cos\vartheta)}\right) \\ + \sum\limits_{i=1}^{l} \gamma f(i) I_{ML} \prod\limits_{j=i+1}^{l} \exp\left(-\dfrac{d(j)}{\lambda'(j) \cos\vartheta}\right), & l \geq l_0. \end{cases} \qquad (12)$$

3. Influence of the transition layer properties on the form of $I(l)$

Expression (12) allows to analyze how the transition layer parameters l_0, l_m and γ affect the form of $I(l)$ for typical REM–Si(111) structures. The analysis results are shown in Figure 2. In this figure, the film thickness region is limited by 0–10 ML, because most significant changes of the interface properties occur in this range during film structure formation process. Dashed lines show $I(l)$ calculated for $\gamma = 0$ (without mixing). Tis case corresponds to the layer-by-layer film growth mode by the FM mechanism. The family of dependences shown by solid lines in Figure 2, *a* has been calculated at fixed $l_0 = 1$ ML and $l_m = 8$ ML, i.e. at permanent transition layer thickness and various mixing coefficients ($\gamma = 0.3$, 0.6, 0.9 and 1.2). It can be seen that the substrate atom diffusion into the metal film restrains the decrease of I with growing coating and results in occurrence of a feature in the form of an „shoulder" on $I(l)$, as mentioned above in Section 1. The intensity of this feature steadily increases with growing number of impurity atoms in the film. For quantitative assessment, the detail shows differential dependences $\Delta I(l)$ calculated by subtraction of $I(l)$ at $\gamma = 0$ from similar curves at $\gamma > 0$. It can be seen that ΔI quickly grows beginning from the smallest coatings and achieves its peak at $l = 4$–5 ML, and then quickly decreases, but does not become equal to zero even at 10 ML.

When the transition layer thickness becomes half as much, i.e. at $l_0 = 1$ ML and $l_m = 4$ ML, the results are qualitatively similar (Figure 2, *b*). The main difference is in that the „shoulder" on $I(l)$ becomes less pronounced, and the peak on $\Delta I(l)$ moves to the smaller coating region (~ 3 ML).

With increasing l_0, the „shoulder" on $I(l)$ is of more abrupt (threshold) nature (Figure 2, *c*). This figure shows the findings obtained at $l_0 = 2$ ML, $l_m = 8$ ML and varying γ. As can be seen, with intense diffusion of substrate atoms into the film (at $\gamma = 1.2$) on $I(l)$, even a small peak can be observed at $l = 2$.

Finally, with varying l_m corresponding to the transition layer thickness increase or decrease, the center of gravity of the „shoulder" moves to the thicker or thinner coating region, respectively. Figure 2, *d* shows the data obtained at $l_0 = 1$ ML, $\gamma = 0.6$ and varying $l_m = 3$, 6, 9, 12 and 15 ML. As shown in the detail, the peak on $\Delta I(l)$ steadily moves to the right with growing l_m.

Thus, the model described herein allows to identify the relation between the form of $I(l)$, on the one hand, and the structure and composition of the transition layer of diffusion interfaces, on the other hand.

4. Quantitative analysis of REM (Yb, Sm, Gd)–Si(111) film structures

In this section, the offered model is used to interpret the experimental findings obtained earlier for the Yb–Si(111) [23], Sm–Si(111) [26] and Gd–Si(111) [21] film structures. These structures have been chosen because $I(l)$ recorded for them show more or less clearly pronounced features in the form of the „shoulder" similar to those described in Section 3. Such dependences were simulated herein using expression (12). For the calculation, the thickness d of one ML of ytterbium, samarium and gadolinium was assumed equal to their atom diameters (3.86, 3.62 and 3.58 Å respectively [30]). The free electron transit length λ in these REM films (the experiments recorded the Auger peak of Si *LVV* with 92 eV) is equal to 3.77 ML [31], which corresponds to 14.55, 13.65 and 13.50 Å. Thickness d_S of one ML of Si atoms was equal to 1.57 Å. Finally, the free electron transit length λ_S in silicon was assumed equal to 5.07 Å [32]. Figure 3–5 shows the simulation of $I(l)$. The experimental data is shown by squares. Design dependences are shown by solid lines and solid circles. These dependences were improved by varying l_0, l_m and γ. Integer values were

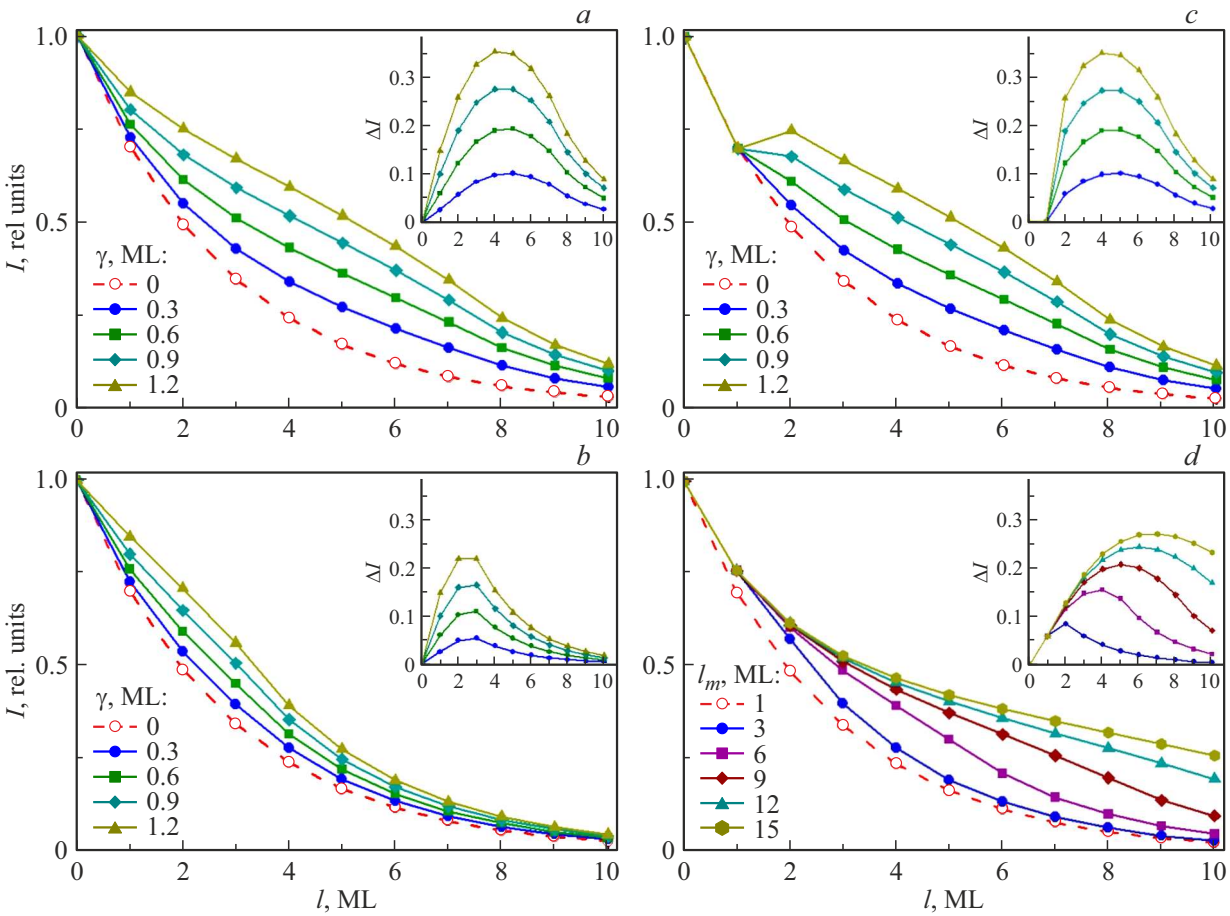

Figure 2. Design relations $I(l)$ for typical REM−Si(111) structures. Auger signal rate I is normalized to I_0. Transition layer parameters: (*a*) $l_0 = 1$ ML, $l_m = 8$ ML, $\gamma = 0$, 0.3, 0.6, 0.9 and 1.2 ML; (*b*) $l_0 = 1$ ML, $l_m = 4$ ML, $\gamma = 0$, 0.3, 0.6, 0.9 and 1.2 ML; (*c*) $l_0 = 2$ ML, $l_m = 8$ ML, $\gamma = 0$, 0.3, 0.6, 0.9 and 1.2 ML; (*d*) $l_0 = 1$ ML, $\gamma = 0.6$ ML, $l_m = 1$, 3, 6, 9, 12 and 15 ML. The details show differential dependences $\Delta I(l)$ determined as the difference of the Auger signals for structures, where mixing takes place, and for structures, where mixing is absent. The thickness of the deposited film atom monolayer is equal to 3.8 Å.

assigned to the first two of them, and arbitrary values were assigned to the mixing coefficient. Improvement was performed until the best agreement between the calculation and experiment was achieved. Parameters at which this agreement was achieved are listed in the table. This table also provides $N_{total} = \sum_{i=1}^{l_m} \gamma f(i)$ equal to the full number of silicon atoms in the transition layer for each of the film structures. Finally, for comparison, Figures 3−5 also show dependences with dashed lines, which are obtained for the case when there is no transition layer at the interface ($\gamma = 0$, FM growth mechanism).

The review of Figures 3−5 immediately suggests that mixing at different rate takes place and a transition layer is formed at the interface in all three REM−silicon systems. Figure 3 and the Table show that for the Yb−Si(111) system the critical metal film thickness, at which substrate atom diffusion starts into the film,is within $1 < l_0 < 2$ ML. Mixing is ended at $l_m = 5$ ML. Taking into account the magnitude of γ (0.65) and the corresponding numerical proportion of Si and Yb atoms ($\sim 3:5$), it can be assumed

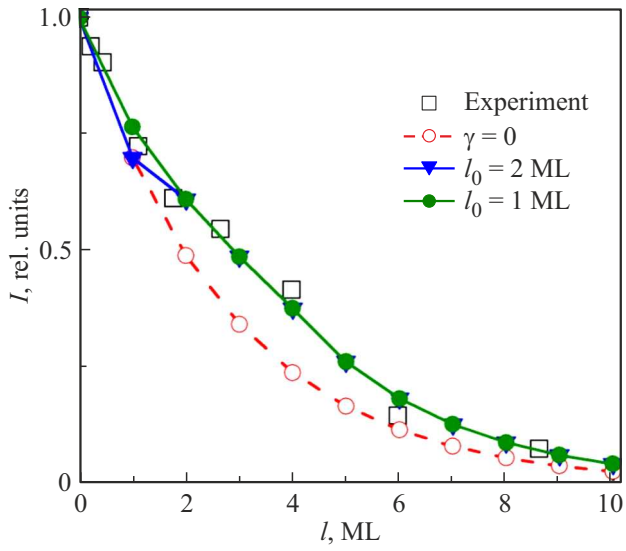

Figure 3. Comparison of experimental and calculated $I(l)$ for the Yb−Si(111) film system. For details see the text. The experimental data was taken from [13].

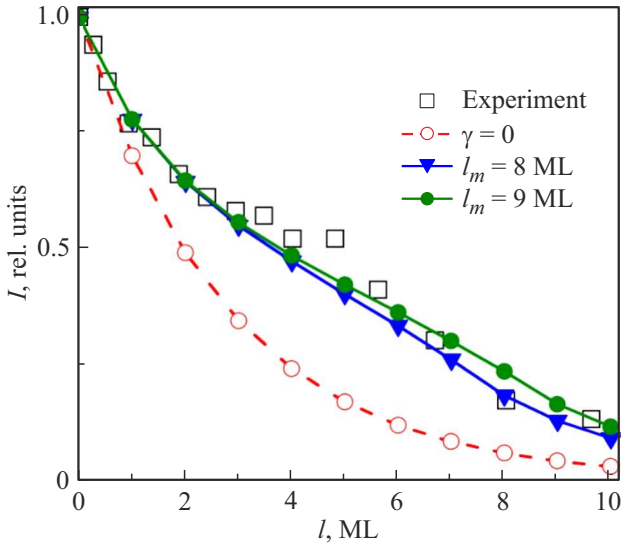

Figure 4. Similar to Figure 3, but for the Sm–Si(111) system. The experimental data was taken from [16].

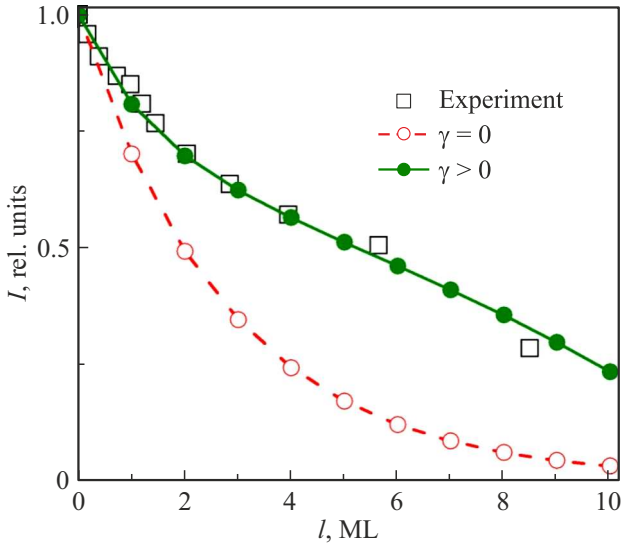

Figure 5. Similar to Figure 3, but for the Gd–Si(111) system. The experimental data was taken from [11].

Transition layer parameters for REM–Si(111) film structures. (The values are expressed in ML. For the Sm–Si(111) structure, averaged N_{total} is given for $l_m = 8$ and 9 ML)

Structure	l_0	l_m	γ	N_{total}
Yb–Si(111)	1–2	5	0.65	1.6
Sm–Si(111)	1	8–9	0.75	3.2
Gd–Si(111)	1	11	1.0	5.5

that ytterbium-enriched Yb_5Si_3 is formed on the interface of the transition layer and silicon substrate. Such compound has the Mn_5Si_3 type structure and is stable at room temperature [33].

In the Sm–Si(111) (Figure 4) and Gd–Si(111) (Figure 5) systems, the critical coating within the model is $l_0 = 1$ ML, and mixing likely starts at lower numbers of REM atoms on the surface. Mixing ends at $l_m = 8$–9 ML and 11 ML, respectively. Thus, the transition layer duration for the three studied interfaces increases in the row Yb → Sm → Gd, which fully agrees with the representations of chemical activity of the listed adsorbates: gadolinium is the most active of them, and ytterbium is the least active.

Similar correlation is also traced when comparing γ for the three listed interfaces. As shown in the Table, it is steadily growing in the ytterbium → samarium → gadolinium row and is equal to 0.65, 0.75 and 1.0, respectively. This may suggest that stable Sm_5Si_4 and GdSi [9] compounds may be formed at the silicon substrate interface in the Sm–Si(111) and Gd–Si(111) systems. For visual comparison of the three interface, Figure 6 shows diagrams illustrating the interface structures and stoichiometric composition.

Finally, correlation of N_{total} (Table) and thermodynamic properties of the deposited REM should be noted. In Figure 7, the vertical axis contains N_{total} values obtained for the Yb–Si(111), Sm–Si(111) and Gd–Si(111) structures herein, and two horizontal axes contain the sublimation heat (upper axis) and melting heat (lower axis) values for ytterbium, samarium and gadolinium listed in [34]. A set of important conclusions may be made from Figure 7. First,

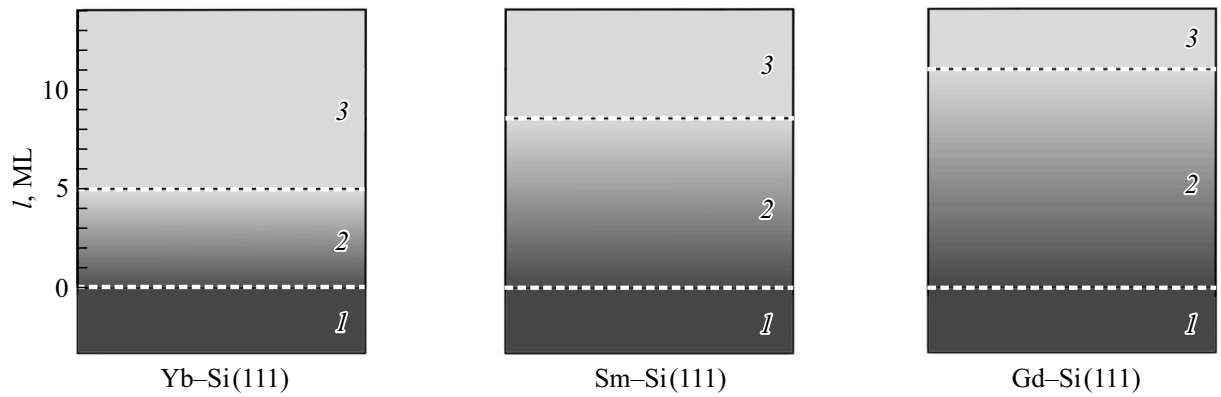

Figure 6. REM (Yb, Sm, Gd)–Si(111) interface models. Numbers denote: *1* — silicon substrate, *2* — transition layer, *3* — metal film.

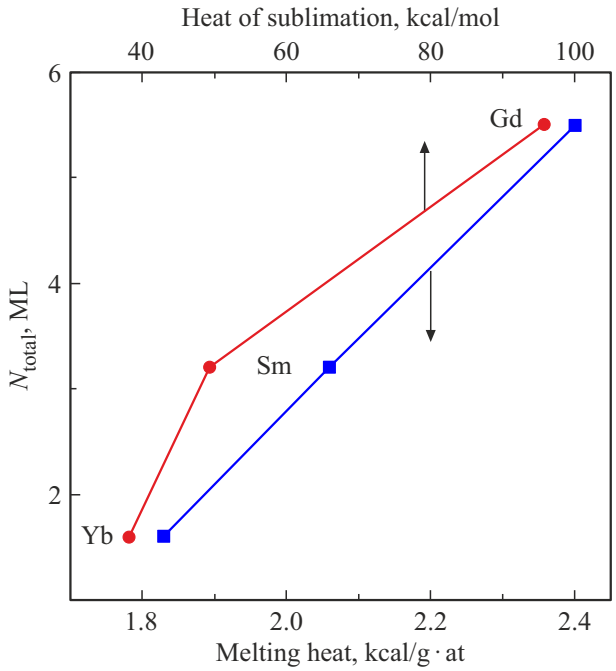

Figure 7. Dependences of N_{total} for the REM (Yb, Sm, Gd)−Si(111) structures (see the Table) on the sublimation heat(upper x axis) and melting heat (lower x axis) of ytterbium, samarium and gadolinium. Sublimation and melting heats are taken from [23].

the number of Si atoms in the transition layer steadily grows with the increasing sublimation and melting heat of the studied REM. Second, the linear nature of the dependence of N_{total} on melting heat is of interest. The mixing mechanism in the REM-silicon structures has not been studied in detail yet. Nevertheless, the findings suggest that phase transition takes place in the growing film at $l = l_0$, for example, film metallization. This transition is followed by energy release proportional to the REM melting heat eventually resulting in interatomic bond breakdown in the silicon substrate and amorphization of surface atomic layers. The latter enables the Si atom diffusion into the metallic film and transition layer formation.

5. Conclusion

A model that describes quantitatively concentration dependences of Auger signals for film system with diffusion interfaces is offered herein. The form of dependences of the Auger signal of the substrate on the deposited film thickness is examined as function of the critical coating l_0, transition layer thickness l_m and mixing parameter γ. To verify the model, calculated and experimental data for the Yb−Si(111), Sm−Si(111) and Gd−Si(111) film systems were compared. This comparison gave the quantitative data characterizing the structure and composition of the listed systems. It is shown that the interface parameters correlate with the thermodynamic properties of the studied REM, in particular, l_m and γ increase in the Yb → Sm → Gd row. The obtained data may be used to make a generalized model of the REM-silicon film structures at room temperature.

Conflict of interest

The authors declare that they have no conflict of interest.

References

[1] L. Feldman, D. Myer. Osnovy analiza poverhnosti i tonkikh plenok. Mir, M. (1989). 342 p. (in Russian)
[2] G.G. Vladimirov. Fizika poverhnosti tverdykh tel. Lan', SPb. (2016). 352 p. (in Russian).
[3] I. Lucci, S. Charbonnier, L. Pedesseau, M. Vallet, L. Cerutti, J.-B. Rodriguez, E. Tournié, R. Bernard, A. Létoublon, N. Bertru, A. Le Corre, S. Rennesson, F. Semond, G. Patriarche, L. Largeau, P. Turban, A. Ponchet, C. Cornet. Phys. Rev. Mater. **2**, 060401-1-6 (2018).
[4] D.J. Eaglesham, M. Cerullo. Phys. Rev. Lett. **64**, 1943 (1990).
[5] R.C. Newman. Phil. Mag. **2**, 750 (1957).
[6] A. Mlynczak, R. Niedermayer. Thin Solid Films **28**, 37 (1975).
[7] R. Kern, G. Le Lay, J.J. Metois. In: Current Topics in Material Science / Ed. E. Kaldis. North-Holland, Amsterdam (1979). V. 3. P. 178.
[8] G. Rossi. Surf. Sci. Rep. **7**, 1 (1987).
[9] F.P. Netzer. J. Phys. Condens. Matter **7**, 991 (1995).
[10] A. Seiler, O. Bauder, S. Ibrahimkutty, R. Pradip, T. Prüßmann, T. Vitova, M. Fiederle, T. Baumbach, S. Stankov. J. Cryst. Growth **407**, 74 (2014).
[11] S. Sanna, C. Dues, W.G. Schmidt, F. Timmer, J. Wollschläger, M. Franz, S. Appelfeller, M. Dähne. Phys. Rev. B **93**, 195407 (2016).
[12] M. Franz, S. Appelfeller, C. Prohl, J. Große, H.-F. Jirschik, V. Füllert, C. Hassenstein, Z. Diemer, M. Dähne. J. Vac. Sci. Technol. A **34**, 061503 (2016).
[13] S. Chandola, E. Speiser, N. Esser, S. Appelfeller, M. Franz, M. Dähne. Appl. Surf. Sci. **399**, 648 (2017).
[14] S. Tanusilp, Y. Ohishi, H. Muta, S. Yamanaka, A. Nishide, J. Hayakawa, K. Kurosaki. Phys. Status Solidi RRL **12**, *2*, 1700372 (2018).
[15] I. Goldfarb, F. Cesura, M. Dascalu. Adv. Mater. **30**, *41*, 1800004 (2018).
[16] A.M. Tokmachev, D.V. Averyanov, I.A. Karateev, O.E. Parfenov, O.A. Kondratev, A.N. Taldenkov, V.G. Storchak. EPJ Web of Conf. **185**, 01010 (2018).
[17] K. Holtgrewe, S. Appelfeller, M. Franz, M. Dähne, S. Sanna. Phys. Rev. B **99**, 214104 (2019).
[18] D.V. Averyanov, I.S. Sokolov, M.S. Platunov, F. Wilhelm, A. Rogalev, P. Gargiani, M. Valvidares, N. Jaouen, O.E. Parfenov, A.N. Taldenkov, I.A. Karateev, A.M. Tokmachev, V.G. Storchak. Nano Res. **13**, 3396 (2020).
[19] A.M. Tokmachev, D.V. Averyanov, A.N. Taldenkov, I.S. Sokolov, I.A. Karateev, O.E. Parfenov, V.G. Storchak. ACS Nano **15**, 12034 (2021).
[20] S. Gokhale, N. Ahmed, S. Mahamuni, V.J. Rao, A.S. Nigavekar, S.K. Kulkarni. Surf. Sci. **210**, 85 (1989).
[21] W.A. Henle, F.P. Netzer, R. Cimino, W. Braun. Surf. Sci. **221**, 131 (1989).

[22] A. Siokou, S. Kennou, S. Ladas. Surf. Sci. **331**–**333**, 580 (1995).
[23] T.V. Krachino, M.V. Kuzmin, M.V. Loginov, M.A. Mitsev. FTT, **39**, 1672 (1997). (in Russian).
[24] A.Yu. Grigoriev, A.M. Shikin, G.V. Prudnikova, S.A. Gorovikov, V.K. Adamchuk. FTT, **40**, 562 (1998). (in Russian).
[25] A.Yu. Grigoriev, A.M. Shikin, G.V. Prudnikova, S.A. Gorovikov, V.K. Adamchuk. Poverkhnost', **8**–**9**, 146 (1998). (in Russian)
[26] T.V. Krachino, M.V. Kuzmin, M.V. Loginov, M.A. Mitsev. FTT, **40**, 1937 (1998). (in Russian).
[27] W.A. Henle, M.G. Ramsey, F.P. Netzer, S. Witzel, W. Braun. Surf. Sci. **243**, 141 (1991).
[28] J. Onsgaard, M. Christiansen, F. Orskov, P.J. Godowski. Surf. Sci. **247**, 208 (1991).
[29] D.V. Buturovich, M.V. Kuzmin, M.V. Loginov, M.A. Mitsev. FTT, **50**, 168 (2008). (in Russian).
[30] Svoistva elementov. Spravochnik. Metallurgiya, M., (1976). Ch. 1.
[31] F. Gerken, J. Barth, R. Kammerer, L.I. Johansson, A. Flodström. Surf. Sci. **117**, 468 (1982).
[32] S. Tanuma, S.J. Powell, D.R. Penn. Surf. Interface Anal. **17**, 911 (1991).
[33] A. Grytsiv, D. Kaczorowski, A. Leithe-Jasper, V.H. Tran, A. Pikul, P. Rogl, M. Potel, H. Noël, M. Bohn, T. Velikanova. J. Solid State Chem. **163**, 178 (2002).
[34] E.M. Savitsky, V.F. Terekhova, Metallovedenie redkozemelnykh metallov. Nauka, M. (1975). 271 p. (in Russian).

Translated by E.Ilyinskaya